

## Sources of particulate organic nitrates in the boreal forest in Finland

Aki Kortelainen<sup>1)</sup>, Liqing Hao<sup>1)\*</sup>, Petri Tiitta<sup>2)</sup>, Antti Jaatinen<sup>1)</sup>, Pasi Miettinen<sup>1)</sup>, Markku Kulmala<sup>3)</sup>, James N. Smith<sup>1)4)</sup>, Ari Laaksonen<sup>1)5)</sup>, Douglas R. Worsnop<sup>1)3)5)6)</sup> and Annele Virtanen<sup>1)</sup>

<sup>1)</sup> Department of Applied Physics, University of Eastern Finland, P.O. Box 1627, FI-70211 Kuopio, Finland (\*corresponding author's e-mail: hao.liqing@uef.fi)

<sup>2)</sup> Department of Environmental Science, University of Eastern Finland, P.O. Box 1627, FI-70211 Kuopio, Finland

<sup>3)</sup> Department of Physics, P.O. Box 64, FI-00014 University of Helsinki, Finland

<sup>4)</sup> Atmospheric Integrated Research, University of California, 1102 Natural Sciences 2, Irvine, CA 92697-2025, USA

<sup>5)</sup> Finnish Meteorological Institute, Research and Development, FI-00101 Helsinki, Finland

<sup>6)</sup> Aerodyne Research Inc., 45 Manning Road, Billerica, MA 01821-3976, USA

Received 15 Mar. 2016, final version received 3 Aug. 2016, accepted 1 Aug. 2016

Kortelainen A., Hao L., Tiitta P., Jaatinen A., Miettinen P., Kulmala M., Smith J.N., Laaksonen A., Worsnop D.R. & Virtanen A. 2017: Sources of particulate organic nitrates in the boreal forest in Finland. *Boreal Env. Res.* 22: 13–26.

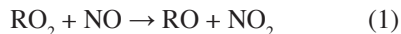
Organic nitrates (ON) are known to be present in secondary organic aerosol and act as a reservoir of nitrogen oxides, regulating the local and regional ozone and hydroxyl radical budgets. This work reports observations of particulate ON in Finnish remote boreal forest at a site with dominant emissions from biogenic volatile organic compounds. High Resolution-Aerosol Mass Spectrometer data were analysed in a unique way to characterize the sources of inorganic and organic nitrates. ON were found to be related to local sources with semi-volatile properties. Also they were implying a nocturnal formation mechanism. Occasionally, local sawmill emissions contributed greatly to the organic nitrates. The observations indicated that in the remote boreal forest area the NO<sub>3</sub> radicals are oxidizing biogenic VOCs producing ON. This work demonstrates the significant impact of anthropogenic-biogenic emissions interaction on the atmospheric organic nitrate aerosol mass concentration.

### Introduction

Atmospheric aerosol particles affect climate directly by scattering and absorbing solar radiation and indirectly by forming cloud condensation nuclei (e.g. IPCC 2013). A better understanding of their atmospheric sources is important for assessing their atmospheric influence and reducing the uncertainties in model simulation of climate change.

Organic nitrates (ON) are known to be present in atmospheric aerosol but are not explored well in spite of their high importance to atmospheric chemistry. Model simulations and experiments both show that ON from oxidation of biogenic volatile organic compounds (VOCs) are a significant contributor to the aerosol in anthropogenically-affected areas (e.g. Pye *et al.* 2010, Rollins *et al.* 2012). The formation of ON in the atmosphere can be achieved via a reaction

of peroxy radicals ( $\text{RO}_2$ ) with NO in the photochemistry:



Photolysis of the major reaction channel 1, lead to ozone formation via a  $\text{NO}_x$  cycle (Atkinson 2000). Channel 2 is a minor pathway that forms ON. ON are also formed from oxidation of VOCs by  $\text{NO}_3$  radicals in the nocturnal chemistry:



Hence ON act as a sink or reservoir of atmospheric  $\text{NO}_x$  ( $\text{NO}$  and  $\text{NO}_2$ ) species. Some ON molecules have lifetimes that are long enough for a regional transport. The importance of ON in regulating the atmospheric ozone and OH budgets locally and regionally has been recognized (Seinfeld and Pandis 2006).

In the last decade, studies of ON formation were conducted both in the laboratory and field. Chamber experiments showed that organic nitrate yields from isoprene oxidation by  $\text{NO}_3$  vary from 4.3% to 23.8% (Ng *et al.* 2008), while the ON production from  $\beta$ -pinene and limonene reactions with  $\text{NO}_3$  reach mass yields of 50% and 30%, respectively (Fry *et al.* 2009, 2011). However, ON from  $\text{NO}_3$  oxidation of  $\alpha$ -pinene lead to zero aerosol formation under dark chemistry (Fry *et al.* 2013), in contrast to a yield of 26% from photochemistry (Rindelaub *et al.* 2014). These results show that the ON formation depends on the VOC precursors, and most probably on the size and structure of these compounds. In ambient environments, particulate organic nitrates are widely detected by thermal dissociation-laser induced fluorescence (TD-LIF) (Day *et al.* 2002) and Fourier transform infrared spectroscopy (Garnes and Allen 2002), both in remote forested and urban areas. The daily variations of ON are strongly controlled by the ambient  $\text{NO}_x$  level (e.g. Browne 2013), day and night chemistry (e.g. Fry *et al.* 2013, Day *et al.* 2009), temperature (e.g. Day *et al.* 2008) and loss from deposition, hydrolysis and further oxidation (Liu *et al.* 2012).

Although a number of ambient measurements of ON have been carried out, their detailed formation mechanisms and sources are still poorly understood. In this study, we present the measurement results of particulate organic nitrate aerosols from Hyytiälä, Finland. The campaign site is representative of a remote boreal forest environment dominated by biogenic emissions, and relatively low aerosol mass loadings and  $\text{NO}_x$  concentrations. New-particle formation and growth are frequently observed at the site (Kulmala 2003, Kulmala *et al.* 2004). In recent years, a few studies focused on real-time particulate chemical composition observations and ON were only briefly mentioned. For example, Allan *et al.* (2006) found high  $m/z$  30 peak occasionally in AMS-derived mass spectra of the Aitken mode at the site in Hyytiälä, which was suggested to be possible fragmentation of organic nitrates ( $\text{NO}^+$ ) or amines (e.g.  $\text{CH}_2\text{NH}_2^+$ ). However, they were not able to confirm the finding due to the low mass resolution of the instrument. Raatikainen *et al.* (2010) applied PMF analysis to Q-AMS observations, revealing organic factors and their properties. They found aged, long-range-transported and highly-oxidized OOA1 (Oxidized Organic Aerosol, also referred to as LV-OOA) factor being less volatile, and a more hygroscopic and less oxidized OOA2 factor (similar to SV-OOA) that is more volatile, representing local and non-hygroscopic aerosol. Similar factors were found by Finessi *et al.* (2012): OOA1 was found to be associated with polluted continental air masses and OOA2 with air masses from north-to-west wind directions from Atlantic Ocean and crossing into Scandinavia. In this study, we used a High resolution Time of Flight Aerosol Mass Spectrometer (HR-TOF-AMS) and PMF analysis by integrating organics and nitrate species for the first time and discovered that at the study site the ON formation was strongly affected by the anthropogenic activity and nighttime chemistry.

## Methods

### Measurement site

The measurements were conducted in southern Finland at the SMEAR II (Station for Measuring

Forest Ecosystem-Aerosol Relations) Hyytiälä station (61°51'N, 24°17'E) (Hari and Kulmala 2005) during the early spring of the year 2011 between 15 Mar. and 20 Apr. The site is located on a hill (180 m a.s.l.) surrounded by boreal forest, mainly consisting of Scots pine, Norway spruce, birch and aspen. In addition, there is agriculture in the vicinity of the site and the village of Juupajoki (population < 2000) is located 6 km SE of the site. The densely-populated city of Tampere lies approx. 50 km SW of the site.

### AMS operation and data processing

During the campaign, the size-resolved non-refractory chemical composition of aerosol particles with vacuum aerodynamic diameter of 50–1000 nm was measured by an Aerodyne HR-TOF-AMS. Detailed descriptions of the instrument, measurement and data processing are given in Jayne *et al.* 2000, Jimenez *et al.* 2003 and DeCarlo *et al.* 2006. The HR-TOF-AMS was operated alternating V and W modes for the ion quantification, with V mode providing better sensitivity and W mode better mass resolution. In front of the AMS inlet, the aerosol samples were dried by a Permapure Nafion® dryer to eliminate the possible effect of water content on the aerosol mass quantification.

The AMS data were processed using SQUIRREL Tof-AMS Data Analysis Toolkit ver. 1.5 and PIKA Tof-AMS HR Analysis ver. 1.1H. In addition, an elemental analysis was processed using APES ver. 1.06 (available from <http://cires.colorado.edu/jimenez-group/ToFAMSResources/ToFSoftware/index.html>) within the Igor Pro software. In the elemental analysis, the O:C ratio was calculated by considering the CHO<sup>+</sup> ion correction (Canagaratna *et al.* 2015). For the calculation of aerosol mass concentration, a constant collection efficiency (CE) of 0.5 was applied to account for the particle loss in the aerodynamic transmission lens and heat vaporizer. The default value of CE was chosen according to comparison of AMS vs. DMPS (Differential Mobility Particle Sizer) volume and relatively low amount of inorganic nitrate (Middlebrook *et al.* 2012). The size range of DMPS for the volume calculation was chosen according to detectable size range of AMS. The

densities of the AMS-derived non-refractory compounds were 1.4 g m<sup>-3</sup> for LV-OOA, 1.2 g m<sup>-3</sup> for SV-OOA, 1.725 g m<sup>-3</sup> for NH<sub>4</sub>NO<sub>3</sub>, 1.769 g m<sup>-3</sup> for (NH<sub>4</sub>)<sub>2</sub>SO<sub>4</sub> (Zhang *et al.* 2005b) and 2.0 g m<sup>-3</sup> for black carbon. The relative ionization efficiencies were the default values for organics (1.4), nitrate (1.1), sulphate (1.2) and chloride (1.3), and for ammonium a value of 2.28 was determined from the calculation of ionization efficiency (IE) calibration procedure.

The data analysis was further performed by applying Positive Matrix Factorization (PMF) technique to the high-resolution mass spectra (Paatero and Tapper 1994, Paatero 1997, Ulbrich *et al.* 2009). In this study, PMF analysis was conducted in a way that organic and error matrices of high-resolution mass spectra were generated in PIKA. The time series and errors of NO<sup>+</sup> and NO<sub>2</sub><sup>+</sup> ions were also integrated into the organic and error matrices for PMF analysis. The combined organic and inorganic matrices were then fitted using the PMF evaluation tool. By using this method, we expected to quantify the formation of particulate organic nitrate in a boreal forest area.

The PMF was evaluated with 1 to 10 factors and Fpeak was varied from -1 to 1. Knowledge of formerly reported mass spectra profiles and supporting measurement data from other instruments and campaigns were used to assist the interpretation of the PMF results. The number of factors was chosen to be three because additional factors did not give extra information for the analysis and because this number explained well enough the outcome and the residuals were low according to the *Q* value of 3.97. The coefficient of determinations (*R*<sup>2</sup>) for Fpeak value of 1 indicated the best correlations between the factors and studied tracers in the chosen Fpeak range (*see* Table 1). Hence, the Fpeak value of 1 was chosen for the final solution.

### Other supporting measurements

The aerosol number concentration and size distributions in a size range of 10–800 nm were measured by a Differential Mobility Particle Sizer (DMPS). The DMPS shared a same sampling line with AMS part of the campaign at a sampling flowrate of 1 l min<sup>-1</sup>. The rest of the campaign

the DMPS was removed and AMS had external pump to keep the sampling flow rate at the same level. Trace gas constituents ( $O_3$ ,  $NO_x$ ,  $SO_2$ ,  $CO$ ,  $CO_2$ ) and meteorological parameters (wind speed, wind direction, precipitation, temperature and relative humidity) were measured continuously at the site and saved in the data archive of the University of Helsinki's Smart-SMEAR data repository (Junninen *et al.* 2009). When the data were available, the averaging time for meteorological parameters and trace gases was chosen to be 1 h and sampling height was 4 m. The relative humidity was measured by an RH sensor (model MPI02H, Rotronic, Switzerland) and precipitation (liquid water equivalent) was recorded as 1-min accumulations. Shortwave solar radiation was measured by a pyranometer (model SK08, Middleton, Australia) in a wavelength range of 0.3–4.8  $\mu\text{m}$ . Black carbon (BC) was measured by an aethalometer (model AE-16, Magee Scientific, Berkeley, CA) that used light-emitting diode at  $\lambda = 880 \text{ nm}$  (Virkkula *et al.* 2007).  $CO_2$  was measured by an infrared light absorption analyser (LI-840 model, Li-Cor, Nebraska, USA),  $CO$  by an infrared light absorption analyser (Horiba APMA model, Horiba Ltd., Japan),  $O_3$  by an ultraviolet absorption analyser (TEI 49 C),  $NO_x$  by a chemiluminescence analyser (TEI 42 CTL, Thermo Fisher Scientific, MA, USA) with photolytic converter and  $SO_2$  by a fluorescence analyser (TEI 43 CTL, Thermo Fisher Scientific, MA, USA). Air trajectories were computed using the HYSPLIT Trajectory Model (Draxler *et al.* 2013, Rolph *et al.* 2013).

## Deriving inorganic molecules

The AMS measures non-refractory organic and inorganic species, such as organics, sulphate

**Table 1.**  $R^2$  values for the Fpeak values of -1, 0, 1 for comparison of species.

	-1	0	1
$R^2$ (LV-OOA vs. $CO_2^+$ )	0.94	0.95	0.98
$R^2$ (LV-OOA vs. estimated $(NH_4)_2SO_4$ )	0.52	0.53	0.60
$R^2$ (SV-OOA vs. Organic $NO_3$ )	0.92	0.99	0.99
$R^2$ (NO-factor vs. est. $NH_4NO_3$ )	0.94	0.94	0.94

( $SO_4^{2-}$ ), nitrate ( $NO_3^-$ ), ammonium ( $NH_4^+$ ) and chloride ( $Cl^-$ ). Based on the principles of aerosol neutralization and molecular thermodynamics, we were able to reconstruct the molecular composition from the ions (McMurry *et al.* 1983). Several neutral molecules such as  $(NH_4)_2SO_4$ ,  $NH_4HSO_4$ ,  $H_2SO_4$ ,  $NH_4NO_3$ ,  $NH_4Cl$  and other possible non-refractory molecular species that evaporate at 600 °C were reconstructed from the AMS data for the comparisons with the PMF results. Several rules were used for the calculations. The back-calculations of molecular compounds were estimated according to the ammonium-to-sulphate molar ratio in a way that all ammonium reacts first with sulphate (McMurry *et al.* 1983, Du *et al.* 2010). First, if  $0 < \text{ratio} < 1$ ,  $NH_4$  exists as the chemical forms of  $H_2SO_4$  and  $NH_4HSO_4$ . Second, if  $1 < \text{ratio} < 2$ ,  $NH_4$  exists as  $(NH_4)_2SO_4$  and  $NH_4HSO_4$ . Third, if  $\text{ratio} > 2$ , then the fraction  $NH_4$  corresponding to twice the amount of  $SO_4$  exists as  $(NH_4)_2SO_4$  and the remaining fraction of  $NH_4$  is associated with  $NO_3$  and  $Cl$ . Fourth, the rest of  $NO_3$ , which is not neutralized by  $NH_4$  is from  $NaNO_3$  or organic nitrate.

## Results and discussion

### Overview

The meteorological parameters ( $T$ ,  $RH$ , precipitation,  $WD$  and  $WS$ ) and the time series of individual AMS species varied greatly during the campaign (Fig. 1). Generally, the total volume concentration measured by AMS was in good agreement with the collocated measurements of DMPS, with a ratio of the AMS volume to the DMPS volume concentration being 0.778. The mean  $\pm$  SD total mass concentration was  $1.8 \pm 1.7 \mu\text{g m}^{-3}$  which was close to the values measured earlier in Hyytiälä using a similar instrument (Allan *et al.* 2006, Raatikainen *et al.* 2010). Organics accounted for 49%, sulphate 22%, ammonium 10%, nitrate 7%, black carbon 11% and chloride < 1% of the particle mass over the campaign period.

The time series of mass concentrations of individual chemical species also varied considerably, especially nitrate and organics which were the main focus of this study. Nitrate and organ-

**Fig. 1.** Relative humidity (RH), precipitation, temperature ( $T$ ), wind direction (WD), wind speed (WS), volume concentration and mass loadings of organics (Org), nitrate ( $\text{NO}_3$ ), sulphate ( $\text{SO}_4$ ), ammonium ( $\text{NH}_4$ ), chloride (Chl) and black carbon (BC) during the spring campaign in 2011.

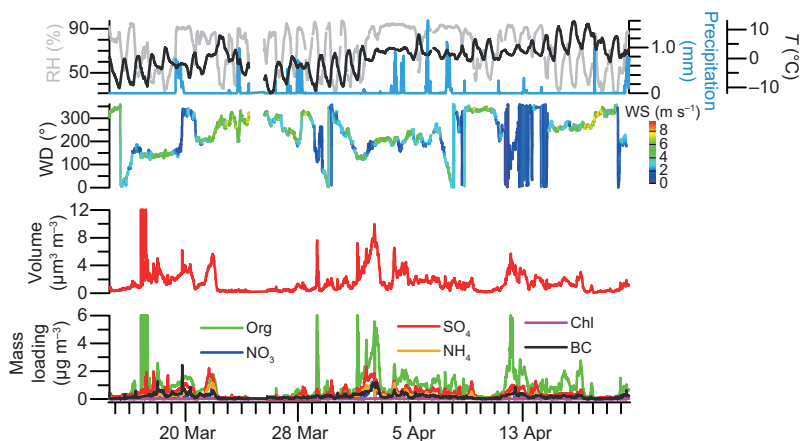
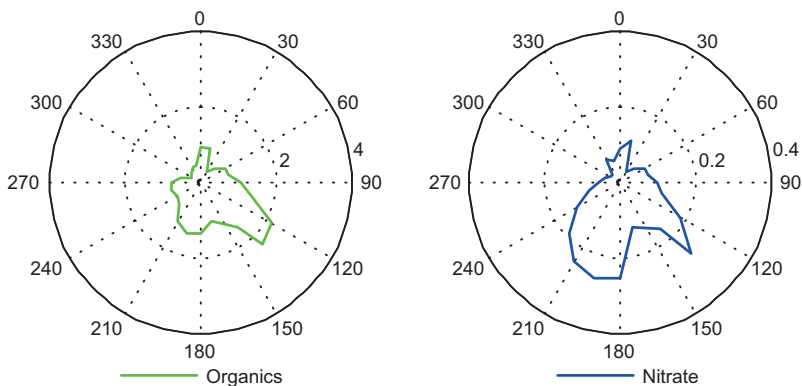


**Fig. 2.** Wind roses of organics and nitrate species (mass loadings  $\mu\text{g m}^{-3}$ ) during the spring campaign.



ics peaked in the direction of  $120^\circ$ – $150^\circ$  which indicated emissions to the southeast (Fig. 2). The direction  $120^\circ$ – $150^\circ$  was consistent with the location of the neighbouring Juupajoki village and especially the local sawmill, which is recognized as an anthropogenic emission sources close to Hyttiälä (Liao *et al.* 2011, Hakola *et al.* 2012, Corrigan *et al.* 2013). Hence, in the following sections, the data are interpreted as with and without the influence of sawmill emissions, which may be representative of an environment in a boreal forest with and without the effect of local anthropogenic activities.

### PMF analysis: Anthropogenic and biogenic sources of organic nitrate

#### PMF results

As mentioned in the prior section, wind from the

direction of  $120^\circ$ – $150^\circ$  brought high amounts of fine particles and other emissions originating from the sawmill to the measurement site during this campaign. By performing PMF analysis on the combined high-resolution organic spectra together with  $\text{NO}^+$  and  $\text{NO}_2^+$  ions for the whole measurement campaign, we identified three factors: SV-OOA, LV-OOA and NO-factor (Fig. 3). Generally, LV-OOA consisted of 54% of the fitted aerosol mass, SV-OOA of 36% and the NO-factor of 10%.

First of all, PMF split the  $\text{NO}^+$  and  $\text{NO}_2^+$  ion fragments into organic and inorganic mass spectra. A separate NO-factor was extracted, which was dominated by the inorganic  $\text{NO}^+$  and  $\text{NO}_2^+$  ions, comprising 88% of the mass of the factor with the remaining species being from organic fragments. The ratio of  $\text{NO}^+/\text{NO}_2^+$  ions in this factor is 2.4, identical to the value for  $\text{NH}_4\text{NO}_3$  determined in the AMS ionization efficiency (IE) calibration procedure. Meanwhile, the time series

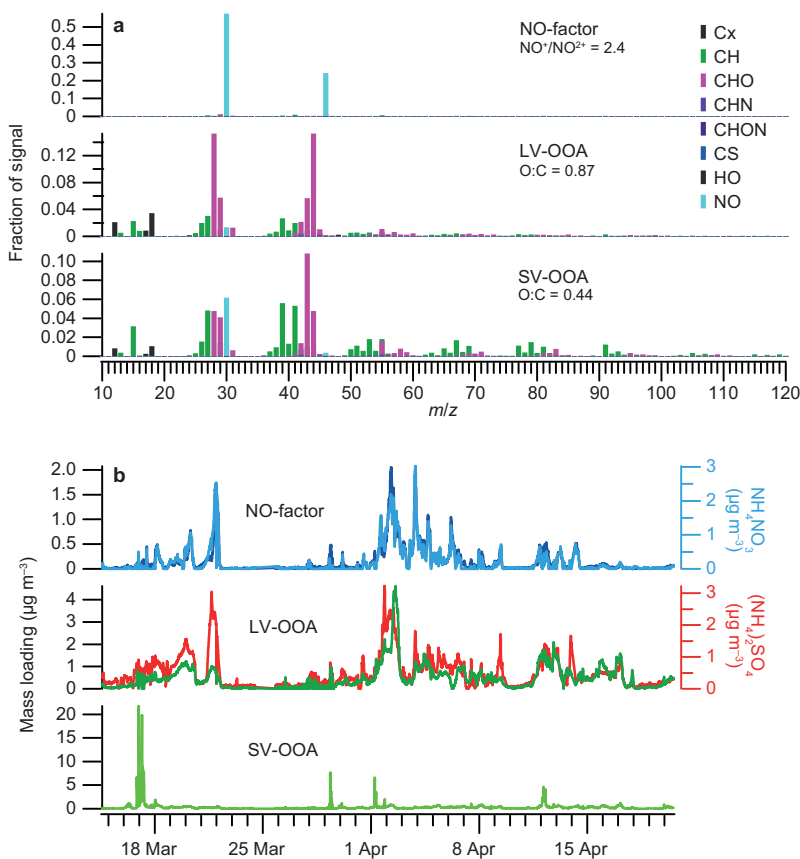


**Fig. 3.** (a) Mass spectra of factors with elemental colouring of ion fragment families and O:C and  $\text{NO}^+/\text{NO}_2^+$  ratios of factors. (b) Mass loadings of NO-factor, LV-OOA, SV-OOA, estimated  $\text{NH}_4\text{NO}_3$  and  $(\text{NH}_4)_2\text{SO}_4$  when the sawmill emissions are included during the spring campaign in 2011.

of this factor was consistent with that of the estimated  $\text{NH}_4\text{NO}_3$  species and, as a consequence, this factor was primarily recognized as a  $\text{NH}_4\text{NO}_3$  inorganic factor. The rest of  $\text{NO}^+$  and  $\text{NO}_2^+$  signal was split into other organic factors in the PMF.

The mass spectral patterns of LV-OOA and SV-OOA were similar to OOA1 and OOA2 components determined by the PMF for the same measurement site (Raatikainen *et al.* 2010) and also resembled the features of LV- and SV-OOA at a global scale (Ng *et al.* 2010). The mass spectrum of SV-OOA was characterized by the prominent peak at  $m/z$  43 ( $\text{C}_2\text{H}_3\text{O}^+$ ). The oxidation level of SV-OOA was represented by an O:C of 0.44. For LV-OOA, it corresponded to more oxidized compounds with a much higher O:C ratio of 0.87. Its mass spectrum was dominated by the peak at  $m/z$  44 ( $\text{CO}_2^+$ ) and  $m/z$  28 ( $\text{CO}^+$ ), comprising 31% of the particulate mass in this factor. As per the chemical composition, the majority of SV-OOA component was roughly comprised of 44% CHO family ions and 45%

CH ions by mass. By contrast, the CHO-family ions made up greater contribution to LV-OOA component (approximately 65% by mass). The time series of LV-OOA showed a good correlation with ammonium sulphate ( $R^2 = 0.6$ ; Fig. 3) and its major sources were the long-ranged transported aerosol from the southern sector, mainly from southern Finland and central Europe based on the wind-rose (Fig. 4) and back-trajectory analyses (Hao *et al.* 2014). For the SV-OOA component, we observed several high mass concentration peaks in the time series. The wind rose showed that these plumes originated from the southeast, where the previously-mentioned sawmill is located. The sawmill has been found to be a significant emission source of anthropogenic monoterpenes at the site (Liao *et al.* 2011, Corrigan *et al.* 2013). Therefore, we hypothesize that the secondary conversation of sawmill emissions was an important anthropogenic source that contributed greatly to the observed SV-OOA component during this study.

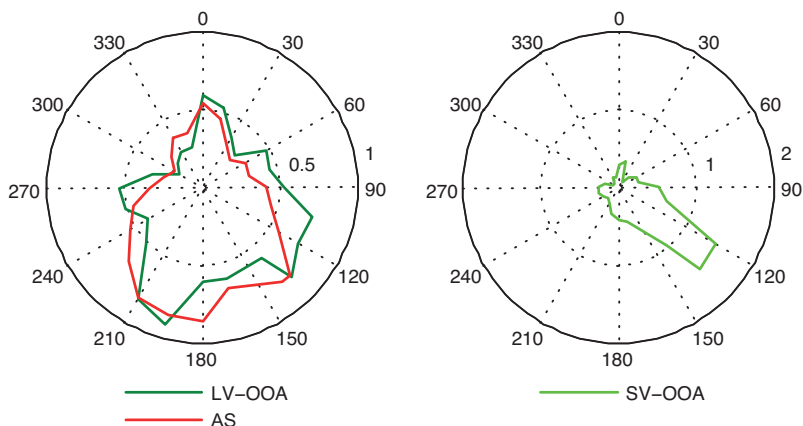


**Fig. 4.** Wind roses of mass loadings ( $\mu\text{g m}^{-3}$ ) LV-OOA, estimated AS  $[(\text{NH}_4)_2\text{SO}_4]$ , and SV-OOA (sawmill-emissions included).

### Determination of particulate organic nitrate

The  $\text{NO}^+$  and  $\text{NO}_2^+$  ions were assigned to different PMF factors due to the different physicochemical properties of nitrate components. Besides the observation of  $\text{NO}_x^+$  ( $\text{NO}^+$  and  $\text{NO}_2^+$ ) ions dominating in NO-factor, we also saw their presence in the organic factors. On average, 65% of the  $\text{NO}_x^+$  family ions were present in the NO-factor, while nearly 30% was from SV-OOA factor and the rest from LV-OOA (Fig. 3). The fact that the assignment of  $\text{NO}_x^+$  ions is split between the inorganic and organic factors implies that nitrate had both organic and inorganic chemical forms. Based on this, we could evaluate the organic nitrates and inorganic nitrates: the  $\text{NO}_x^+$  ions in the NO-factor were used to derive the inorganic nitrate and those in organic factors (SV-OOA and LV-OOA) for determining the organic nitrates.

Total nitrates ( $\text{NO}_3^-$ ) were calculated as a sum of ion fragments of  $\text{N}^+$ ,  $\text{NO}^+$  and  $\text{NO}_2^+$  in AMS. The mass fraction of  $\text{N}^+$  was found to be negligible (approximately 4%), and hence the ratio  $(\text{NO}^+ + \text{NO}_2^+)/(\text{N}^+ + \text{NO}^+ + \text{NO}_2^+)$  was 0.96. Because of its relatively low abundance in total nitrate,  $\text{N}^+$  was not used in the PMF analysis but it was used as a coefficient for calculation of final absolute values of organic and inorganic nitrates. The calculations of organic and inorganic nitrates were performed as follows:

$$\text{NO}_{\text{Org}}^+ = \text{NO}^+_{\text{SV-OOA}} + \text{NO}^+_{\text{LV-OOA}} \quad (5)$$

$$\text{NO}_{2\text{Org}}^+ = \text{NO}_2^+_{\text{SV-OOA}} + \text{NO}_2^+_{\text{LV-OOA}} \quad (6)$$

$$\text{NO}_{\text{Inorg}}^+ = \text{NO}^+_{\text{NO-factor}} \quad (7)$$

$$\text{NO}_{2\text{Inorg}}^+ = \text{NO}_2^+_{\text{NO-factor}} \quad (8)$$

$$\text{NO}_{3,\text{Org}} = (\text{NO}_{\text{Org}}^+ + \text{NO}_{2\text{Org}}^+)/0.96 \quad (9)$$

$$\text{NO}_{3,\text{Inorg}} = (\text{NO}_{\text{Inorg}}^+ + \text{NO}_{2\text{Inorg}}^+)/0.96 \quad (10)$$

where  $\text{NO}_{3,\text{Org}}$  and  $\text{NO}_{3,\text{Inorg}}$  are the organic and inorganic nitrate masses, respectively.  $\text{NO}_{\text{Org}}^+$  and  $\text{NO}_{2\text{Org}}^+$  are the mass concentrations of  $\text{NO}^+$  and  $\text{NO}_2^+$  ions, respectively, in the SV-OOA and LV-OOA factors, while  $\text{NO}_{\text{Inorg}}^+$  and  $\text{NO}_{2\text{Inorg}}^+$  are the corresponding ions in the NO-factor. The four remaining variables can be obtained directly from the PMF results.

In the calculation, particulate organic nitrates refer to the nitrate functional groups ( $-\text{ONO}_2$ ) in this study, which exist in organic molecular forms. The terminology of organic nitrates same as in several previous studies (Day *et al.* 2010, Fry *et al.* 2009, 2011), but different from the one used in some other studies, where organic nitrates refer to the molecules in form of peroxy-nitrates ( $\text{RO}_2-\text{NO}_2$ ) or alkyl nitrates ( $\text{RO}-\text{NO}_2$ ) (e.g. Beaver *et al.* 2012). The relative ionization efficiency of organic nitrate species was set to 1.1, assuming that they are ionized at the same efficiency as  $\text{NH}_4\text{NO}_3$  (Fry *et al.* 2011, Hao *et al.* 2014).

The mean  $\pm$  SD mass concentration of organic nitrates was  $0.033 \pm 0.057 \mu\text{g m}^{-3}$ . Of the total organic nitrate mass loading, 77.7% was assigned to the SV-OOA component, suggesting its semi-volatile nature. This was in line with the results presented by Fry *et al.* (2009) and Hao *et al.* (2014) who studied the organic nitrate species formed from  $\beta$ -pinene oxidation with nitrate radicals in a chamber experiment, and particulate

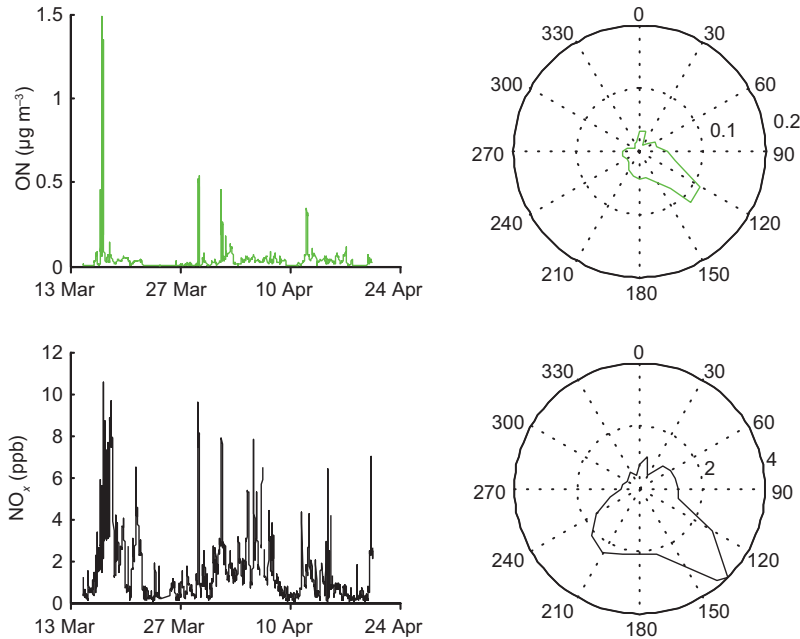


**Fig. 5.** Time series and wind roses of the organic nitrates ( $\mu\text{g m}^{-3}$ ) and  $\text{NO}_x$  (ppb) during the spring campaign in 2011 when the sawmill emission were included.

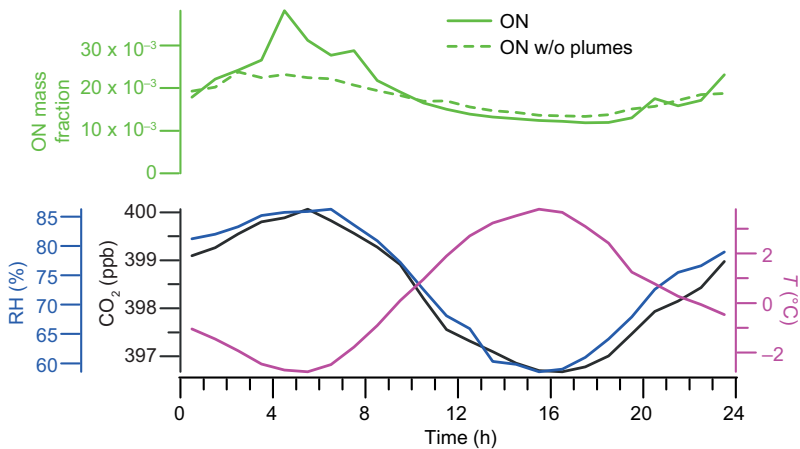


**Fig. 6.** Diurnal cycles of organic nitrate mass fraction (ON) with and without the air mass from wind directions of  $120^\circ$ – $150^\circ$ . The maximum (solid green line) is as a result of sawmill emissions. Gaseous  $\text{CO}_2$  represents an indicator of boundary layer depth variation. Temperature cycle is added to indicate sunlight effect on photochemistry and RH cycle to indicate a possible hydrolysis effect.

organic nitrates in a field experiment, respectively. Meanwhile, we also observed that 22.3% of the organic nitrates were associated with LV-OOA. A wind rose showed a much higher mass concentration of ON in the direction of the sawmill in Juupajoki, matching well with the rose pattern of  $\text{NO}_x$  gas species (Fig. 5). The ON also display a pronounced diurnal cycle that was characterized by a peak at 05:00 and a minimum at 16:00 (Fig. 6). The average mass concentration during the nighttime was roughly double that during the day, suggesting the nocturnal formation as a major source for ON. Hence, we

concluded that the major formation pathways of ON in Hyttiälä was from the reaction between the monoterpene compounds emitted from the sawmill (Liao *et al.* 2011) and the anthropogenic  $\text{NO}_3$  radical (as the results of the reaction of  $\text{NO}_2$  and  $\text{O}_3$ ). In general, 88% of the observed particulate nitrate compounds from the sawmill were composed of organic nitrate, highlighting the importance of anthropogenic activities to the atmospheric nitrate formation. Since the nitrate aerosol in this direction was dominated by organic nitrate, the size distribution of nitrate can well present the distribution of organic

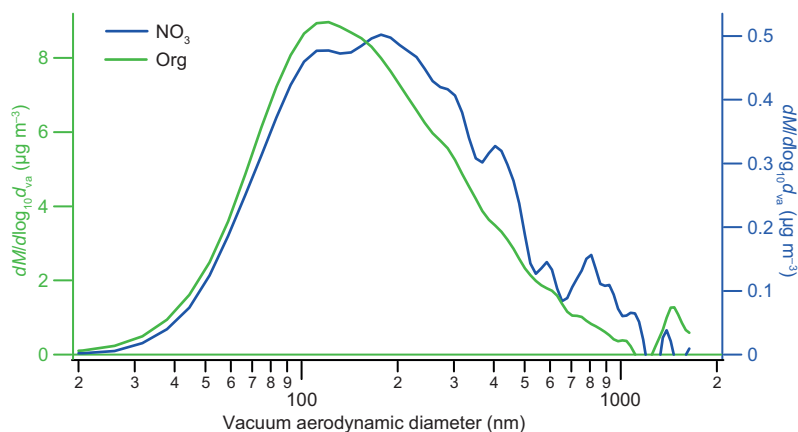


**Fig. 7.** Size distributions of Org and  $\text{NO}_3$  during the sawmill plume.

nitrate. The organic and organic nitrate aerosols exhibited a wide size distribution ranging from 30 nm to around 1000 nm of the vacuum aerodynamic diameter with a mode diameter peaking roughly at 100 nm (Fig. 7). The similarity in the size distributions suggests the same origin of two components.

#### PMF analysis: Biogenic sources of organic nitrate

Based on the wind rose analysis, it was obvious that the SV-OOA and NO factors were greatly affected by the sawmill emissions. To exclude this anthropogenic source from the analysis, we excluded the wind directions from the sector of  $120^\circ$ – $150^\circ$ .

After excluding the sawmill plumes from the data set, we obtained a three-factor solution in the PMF analysis (Fig. 8). The PMF extracted one separate NO-factor and two organic factors, SV-OOA and LV-OOA. The mass spectra of the three factors were very similar to those with the sawmill plumes were included. The NO-factor mass concentration was consistent with the calculated  $\text{NH}_4\text{NO}_3$  compounds in the time series and thus was recognized as a NO-factor with a  $\text{NO}^+/\text{NO}_2^+$  ratio of 2.4. We observed much lower mass concentration for the NO-factor and SV-OOA without the sawmill contribution, but their time series in two cases followed nicely each other with the exception of few plumes. These results again are consistent with our hypothesis that sawmill emissions

are an important, local anthropogenic source that contributes notably to the secondary aerosol formation in Hyytiälä. In contrast, the mass concentrations of LV-OOA component in these two cases were similar, suggesting that LV-OOA is not affected by the local anthropogenic emissions and is originated from regional-transported biogenic species.

Quantification of the ON species without the sawmill emissions was conducted by using the method described earlier. The ON mass concentration varied notably in time (Fig. 9). The mean  $\pm$  SD mass concentration of ON was  $0.027 \pm 0.028 \mu\text{g m}^{-3}$ , which represents a background concentration of ON in the boreal forest in Hyytiälä. The ON mass concentration was slightly lower than the one with the sawmill plumes taken into account ( $0.033 \pm 0.057 \mu\text{g m}^{-3}$ ). Generally, 95% of the ON mass concentration was associated with SV-OOA, implying a dominant secondary formation mechanism for the observed ON in this study. Meanwhile, we saw 5% ON existing in the LV-OOA factor, indicating some ON species have lifetime that are long enough to be transported regionally to the Hyytiälä area.

The diurnal pattern of ON without the sawmill plumes was studied in detail (Fig. 6). We used the measured gaseous  $\text{CO}_2$  as a tracer to indicate the variation of boundary layer depth. Generally, the change of  $\text{CO}_2$  concentration caused by the boundary layer mixing was only around 1%, even though we cannot rule out other possible effects on its concentration. The ON cycle showed a maximum at 02:00 and a minimum in the after-

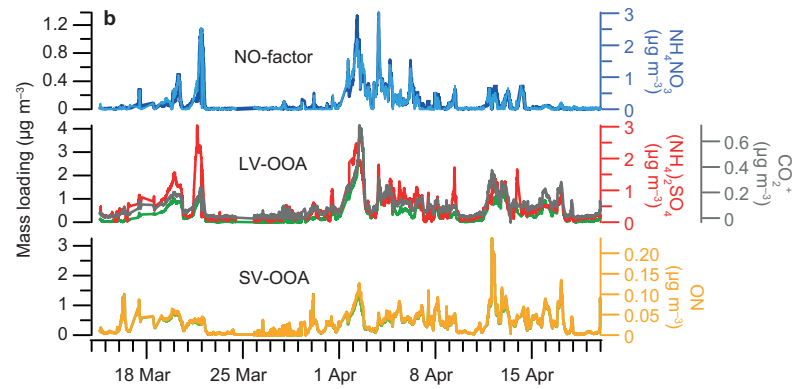
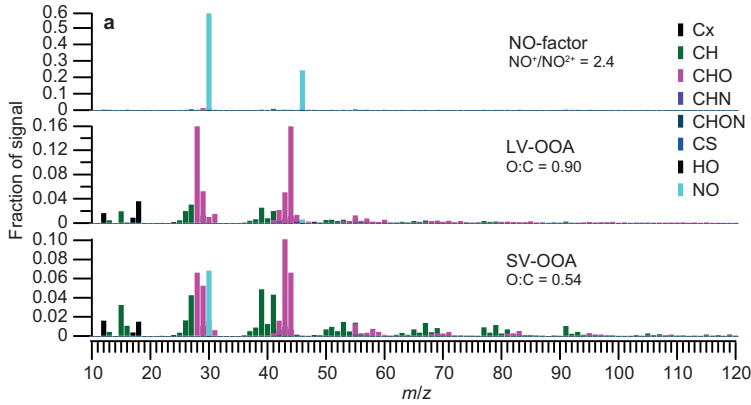


**Fig. 8.** (a) Mass spectra of factors with elemental colouring of ion fragment families and O:C and NO<sup>+</sup>/NO<sub>2</sub><sup>+</sup> ratios of factors. (b) Mass loadings of NO-factor, estimated NH<sub>4</sub>NO<sub>3</sub>, LV-OOA, and estimated (NH<sub>4</sub>)<sub>2</sub>SO<sub>4</sub>, CO<sub>2</sub><sup>+</sup>, SV-OOA and ON at the absence of the sawmills influence during the spring campaign in 2011.

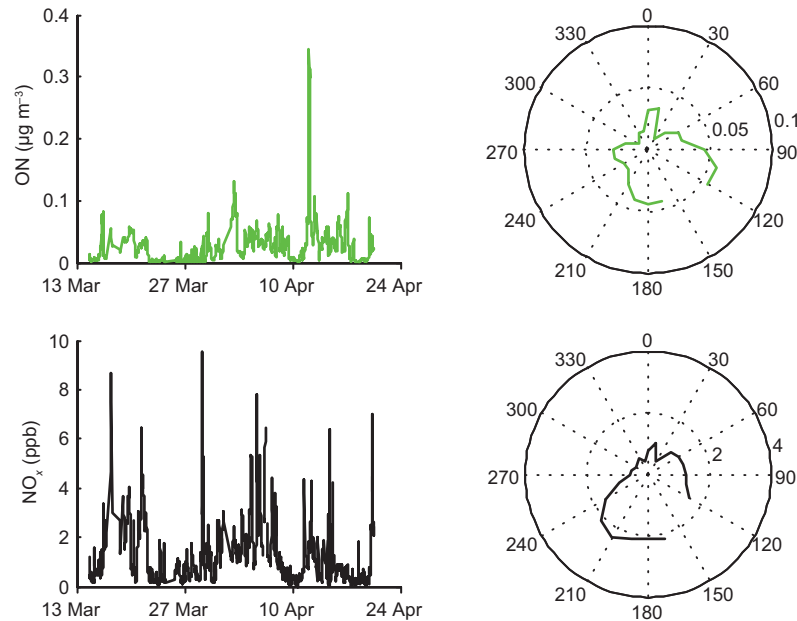


**Fig. 9.** Time series and wind roses of ON ( $\mu\text{g m}^{-3}$ ) and gaseous NO<sub>x</sub> (ppb) during the spring campaign in 2011 with the emissions from the sawmill excluded.

noon. The difference (by a factor of 1.6) in the mass concentrations between the day and night values cannot be interpreted only by the mixing

layer change. Temperature can be another explanation because ON in this study were mainly semi-volatile in nature. Condensation of organic

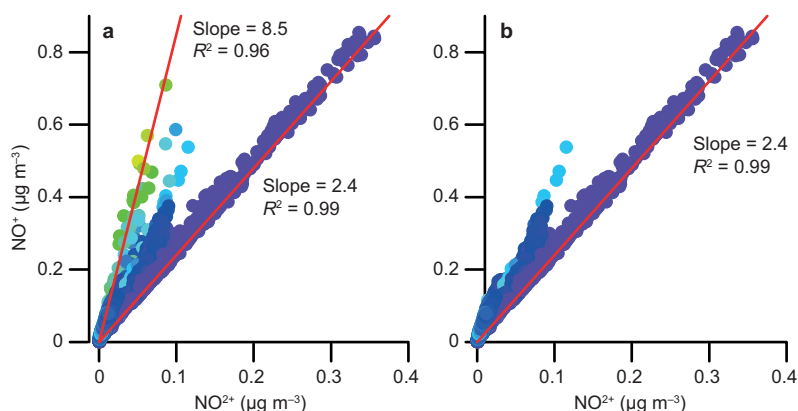


**Fig. 10.** (a)  $\text{NO}^+$  vs.  $\text{NO}_2^+$  colored by ratio of measured  $\text{NH}_4$  and predicted  $\text{NH}_4$ , (b) wind directions of  $120^\circ$ – $150^\circ$  filtered.

nitrate compounds from the gas phase may be enhanced after sunset and particulate ON may evaporate during the day. However, by taking into account a very slight change in temperature (roughly  $6^\circ\text{C}$ ) in Hyytiälä, it was still unlikely that temperature played a key role in the ON variation. Thereby, we can expect that ON were produced via a nocturnal chemistry mechanism due to the observation of a much higher mass concentration during the nighttime, as Raatikainen *et al.* (2010) and Allan *et al.* (2006) report the major production of semi-volatile aerosol during the nighttime in Hyytiälä area.

Based on the analysis, we hypothesize that the ON formation in Hyytiälä was an outcome of the oxidation of biogenic VOC emissions from the boreal forest with anthropogenic oxidants (e.g.  $\text{NO}_3$  radical). Notable particulate organic nitrate formation from nocturnal oxidation was observed in several studies, e.g., in Puijo, which is located in Finland 210 km from SMEAR II (Hao *et al.* 2014), in the Colorado Rocky Mountains (Fry *et al.* 2013), and other remote/rural sites (Rollins *et al.* 2012, Murphy *et al.* 2006). The formation of particulate organic nitrates from  $\text{NO}_3$  radicals during the day is minor due to the rapid decomposition of  $\text{NO}_3$  radical under UV irradiation. However, its formation may be possible from NO termination by peroxy radicals ( $\text{RO}_2$ ) under photochemistry. On one hand, ON observed during the day comes as a residual of prior night products. On the other hand, we are unable to rule out the simultaneous formation of ON compounds during the day via a photochemistry in Hyytiälä.

### $\text{NO}^+/\text{NO}_2^+$ ratio

The difference in the ratios of  $\text{NO}^+/\text{NO}_2^+$  ions has been reported for different nitrate species. In this study, we found that the NO-factor represented mainly ammonium nitrate. The  $\text{NO}^+/\text{NO}_2^+$  ratio in this factor was 2.4 (Fig. 10) and depended on instrument settings, which is consistent with the recent studies reporting the ratios in the range 2–3 (Alfarra *et al.* 2006, Fry *et al.* 2009, Liu *et al.* 2012). The  $\text{NO}^+/\text{NO}_2^+$  ratio of organic nitrates was 8.5, close to the values of laboratory-produced organic nitrates (Fry *et al.* 2009, Farmer *et al.* 2010, Bruns *et al.* 2010) and measured in the field (Farmer *et al.* 2010, Hao *et al.* 2014). Thereby, the  $\text{NO}^+/\text{NO}_2^+$  ratio can be used to estimate the chemical form of nitrate in ambient air. Note that the other forms of nitrate such as sodium nitrate ( $\text{NaNO}_3$ ) produces a high  $\text{NO}^+/\text{NO}_2^+$  ratio of 80 in the AMS mass spectrum (Liu *et al.* 2012), which can interfere with the differentiation of nitrate species. Thus a specific attention should be paid to the nitrate sources at different measurement sites when using the above method.

### Conclusions

Here characterised atmospheric particulate organic nitrate components at a boreal-forest site in Hyytiälä, Finland. The PMF analysis of the unified organic matrices with  $\text{NO}_x^+$  ions was successful in distinguishing the organic and inorganic factors in this study. Of the total

particulate organic nitrates, 77.7% were residing in the SV-OOA factor, suggesting that they were mainly formed from local sources and were semi-volatile in nature. The sawmill, as a local anthropogenic source nearby the measurement site, affected greatly the SV-OOA and organic nitrate formation. After excluding the sawmill plumes, the average mass concentration of organic nitrates was  $0.027 \mu\text{g m}^{-3}$ . In conditions typical for a boreal forest environment (i.e. sawmill plumes excluded from the analysis), the amount of organic nitrates during the night was approximately 1.6 times higher than during the day. Based on these results, we conclude that the organic nitrate formation during our campaign was mainly from the nocturnal oxidation of VOC (either biogenic VOCs from forest emissions or anthropogenic VOCs from sawmill) with anthropogenic oxidant, nitrate radical. This work demonstrates the significant effect of anthropogenic-biogenic emissions interaction on the atmospheric organic nitrate aerosol mass concentration.

*Acknowledgements:* The financial support by the Academy of Finland Centre of Excellence program (decision no. 272041), Academy of Finland (grant no. 259005), European Research Council (starting grant 355478) and strategic funding of the University of Eastern Finland are gratefully acknowledged. L. Hao acknowledges the financial support from UEF Post-doc Research Foundation (930275). The authors gratefully acknowledge the NOAA Air Resources Laboratory (ARL) for the provision of the HYSPLIT transport and dispersion model (<http://www.ready.noaa.gov>).

## References

- Aiken A.C., DeCarlo P.F. & Jimenez J.L. 2007. Elemental analysis of organic species with electron ionization high-resolution mass spectrometry. *Anal. Chem.* 79: 8350–8358.
- Aiken A.C., DeCarlo P.F., Kroll J.H., Worsnop D.R., Huffman J.A., Docherty K.S., Ulbrich I.M., Mohr C., Kimmel J.R., Sueper D., Sun Y., Zhang Q., Trimborn A., Northway M., Ziemann P.J., Canagaratna M.R., Onasch T.B., Alfarra M.R., Prevot A.S.H., Dommen J., Duplissy J., Metzger A., Baltensperger U. & Jimenez J.L. 2008. O/C and OM/OC ratios of primary, secondary, and ambient organic aerosols with high resolution time-of-flight aerosol mass spectrometry. *Environ. Sci. Technol.* 42: 4478–4485.
- Alfarra M.R., Paulsen D., Gysel M., Garforth A.A., Dommen J., Prevot A.S.H., Worsnop D.R., Baltensperger U. & Coe H. 2006. A mass spectrometric study of secondary organic aerosols formed from the photooxidation of anthropogenic and biogenic precursors in a reaction chamber. *Atmos. Chem. Phys.* 6: 5279–5293.
- Allan J.D., Alfarra M.R., Bower K.N., Coe H., Jayne J.T., Worsnop D.R., Aalto P.P., Kulmala M., Hyötyläinen T., Cavalli F. & Laaksonen A. 2006. Size and composition measurements of background aerosol and new particle growth in a Finnish forest during QUEST 2 using an Aerodyne Aerosol Mass Spectrometer. *Atmos. Chem. Phys.* 6: 315–327.
- Atkinson R. 2000. Atmospheric chemistry of VOCs and  $\text{NO}_x$ . *Atmos. Environ.* 34: 2063–2101.
- Beaver M.R., St.Clair J.M., Paulot F., Spencer K.M., Crouse J.D., LaFranchi B.W., Min K.E., Pusede S.E., Wooldridge P.J., Schade G.W., Park C., Cohen R.C. & Wennberg P.O. 2012. Importance of biogenic precursors to the budget of organic nitrates: observations of multifunctional organic nitrates by CIMS and TD-LIF during BEARPEX 2009. *Atmos. Chem. Phys.* 12: 5773–5785.
- Bond T. & Bergstrom R. 2006. Light absorption by carbonaceous particles: an investigative review. *Aerosol. Sci. Tech.* 40: 27–67.
- Browne E.C., Min K.E., Wooldridge P.J., Apel E., Blake D.R., Brune W.H., Cantrell C.A., Cubison M.J., Diskin G.S., Jimenez J.L., Weinheimer A.J., Wennberg P.O., Wisthaler A. & Cohen R.C. 2013. Observations of total  $\text{RONO}_2$  over the boreal forest:  $\text{NO}_x$  sinks and  $\text{HNO}_3$  sources. *Atmos. Chem. Phys.* 13: 4543–4562.
- Bruns E., Perraud V., Zelenyuk A., Ezell M., Johnson S.N., Yu Y., Imre D., Finlayson-Pitts B. & Alexander M.L. 2010. Comparison of FTIR and particle mass spectrometry for the measurement of particulate organic nitrates. *Environ. Sci. Technol.* 44: 1056–1061.
- Canagaratna M.R., Jimenez J.L., Kroll J., Chen Q., Kessler S., Massoli P., Hildebrandt Ruiz L., Fortner E., Williams L., Wilson K., Surratt J., Donahue N., Jayne J.T. & Worsnop D.R. 2015. Elemental ratio measurements of organic compounds using aerosol mass spectrometry: characterization, improved calibration, and implications. *Atmos. Chem. Phys.* 15: 253–272.
- Corrigan A.L., Russell L.M., Takahama S., Äijälä M., Ehn M., Junninen H., Rinne J., Petäjä T., Kulmala M., Vogel A. L., Hoffmann T., Ebben C.J., Geiger F.M., Chhabra P., Seinfeld J.H., Worsnop D.R., Song W., Auld J. & Williams J. 2013. Biogenic and biomass organic aerosol in a boreal forest at Hyytiälä, Finland, during HUMPPA-COPEC 2010. *Atmos. Chem. Phys.* 13: 12233–12256.
- Day D.A., Wooldridge P.J., Dillon M.B., Thornton J.A. & Cohen R.C. 2002. A thermal dissociation laser-induced fluorescence instrument for in situ detection of  $\text{NO}_2$ , peroxy nitrates, alkyl nitrates, and  $\text{HNO}_3$ . *J. Geophys. Res.* 107, D6, 4046, doi:10.1029/2001JD000779.
- Day D.A., Wooldridge P.J. & Cohen R.C. 2008. Observations of the effects of temperature on atmospheric  $\text{HNO}_3$ ,  $\Sigma\text{ANs}$ ,  $\Sigma\text{PNs}$ , and  $\text{NO}_x$ : evidence for a temperature-dependent  $\text{HO}_x$  source. *Atmos. Chem. Phys.* 8: 1867–1879.
- Day D.A., Farmer D.K., Goldstein A.H., Wooldridge P.J., Minejima C. & Cohen R.C. 2009. Observations of  $\text{NO}_x$ ,

- ΣPNs, ΣANs, and HNO<sub>3</sub> at a rural site in the California Sierra Nevada Mountains: summertime diurnal cycles. *Atmos. Chem. Phys.* 9: 4879–4896.
- Day D.A., Liu S., Russell L.M. & Ziemann P.J. 2010. Organonitrate group concentrations in submicron particles with high nitrate and organic fractions in coastal southern California. *Atmos. Environ.* 44: 1970–1979.
- DeCarlo P.F., Kimmel J.R., Trimborn A., Northway M.J., Jayne J.T., Aiken A.C., Gonin M., Fuhrer K., Horvath T., Docherty K., Worsnop D.R. & Jimenez J.L. 2006. Field-deployable, high-resolution, time-of-flight Aerosol Mass Spectrometer. *Anal. Chem.* 78: 8281–8289.
- Draxler R.R. & Rolph G.D. 2013. *HYSPLIT (Hybrid Single-Particle Lagrangian Integrated Trajectory)*. NOAA Air Resources Laboratory, College Park, MD. [Available at <http://www.arl.noaa.gov/HYSPLIT.php>].
- Du H., Kong L., Cheng T., Chen J., Yang X., Zhang R., Han Z., Yan Z. & Ma Y. 2010. Insights into ammonium particle-to-gas conversion: non-sulfate ammonium coupling with nitrate and chloride. *Aerosol Air Quality Res.* 10: 589–595.
- Englund F. & Nussbaum R.M. 2000. Monoterpenes in Scots pine and Norway spruce and their emission during kiln drying. *Holzforschung* 54: 449–456.
- Farmer D.K., Matsunaga A., Docherty K.S., Surratt J.D., Seinfeld J.H., Ziemann P.J. & Jimenez J.L. 2010. Response of the Aerosol Mass Spectrometer to organonitrates and organosulfates and implications for field studies. *Proc. Natl. Acad. Sci. USA* 107: 6670–6675.
- Finessi E., Decesari S., Paglione M., Giulianelli L., Carbone S., Gilardoni S., Fuzzi S., Saarikoski S., Raatikainen T., Hillamo R., Allan J., Mentel Th.F., Tiitta P., Laaksonen A., Petäjä T., Kulmala M., Worsnop D.R. & Facchini M.C. 2012. Determination of the biogenic secondary organic aerosol fraction in the boreal forest by AMS and NMR measurements. *Atmos. Chem. Phys.* 12: 941–959.
- Fry J.L., Kiendler-Scharr A., Rollins A.W., Wooldridge P.J., Brown S.S., Fuchs H., Dubé W.P., Dal Maso M., Tillmann R., Dorn H.-P., Brauers T. & Cohen R.C. 2009. Organic nitrate secondary organic aerosol yield from NO<sub>3</sub> oxidation of β-pinene evaluated using a gas-phase kinetics/aerosol partitioning model. *Atmos. Chem. Phys.* 9: 1431–1449.
- Fry J.L., Kiendler-Scharr A., Rollins A.W., Brauers T., Brown S.S., Dorn H.-P., Dubé W.P., Fuchs H., Mensah A., Rohrer F., Tillmann R., Wahner A., Wooldridge P. J. & Cohen R.C. 2011. SOA from limonene: role of NO<sub>3</sub> in its generation and degradation. *Atmos. Chem. Phys.* 11: 3879–3894.
- Fry J.L., Draper D.C., Zarzana K.J., Campuzano-Jost P., Day D.A., Jimenez J.L., Brown S.S., Cohen R.C., Kaser L., Hansel A., Cappellin L., Karl T., Hodzic Roux A., Turnipseed A., Cantrell C., Lefer B.L. & Grossberg N. 2013. Observations of gas- and aerosol-phase organic nitrates at BEACHON-RoMBAS 2011. *Atmos. Chem. Phys.* 13: 8585–8605.
- Games L.A. & Allen D.T. 2002. Size distributions of organonitrates in ambient aerosol collected in Houston, Texas. *Aerosol Sci. Technol.* 36: 983–992.
- Geng L., Cole-Dai J., Alexander B., Erbland J., Savarino J., Schauer A.J., Steig E.J., Lin P., Fu Q. & Zatzko M.C. 2014. On the origin of the occasional spring nitrate peak in Greenland snow. *Atmos. Chem. Phys.* 14: 13361–13376.
- Granström K. 2003. Emissions of monoterpenes and VOCs during drying of sawdust in a spouted bed. *Forest Products Journal* 53: 48–55.
- Hakola H., Hellén H., Tarvainen V., Bäck J., Patokoski J. & Rinne J. 2009. Annual variations of atmospheric VOC concentrations in a boreal forest. *Boreal Env. Res.* 14: 722–730.
- Hakola H., Hellén H., Hemmilä M., Rinne J. & Kulmala M. 2012. In situ measurements of volatile organic compounds in a boreal forest. *Atmos. Chem. Phys.* 12: 11665–11678.
- Hao L., Romakkaniemi S., Kortelainen A., Jaatinen A., Portin H., Miettinen P., Komppula M., Leskinen A., Virtanen A., Smith J.N., Sueper D., Worsnop D.R., Lehtinen K.E.J. & Laaksonen A. 2013. Aerosol chemical composition in cloud events by high resolution time-of-flight aerosol mass spectrometry. *Environ. Sci. Technol.* 47: 2645–2653.
- Hao L.Q., Kortelainen A., Romakkaniemi S., Portin H., Jaatinen A., Leskinen A., Komppula M., Miettinen P., Sueper D., Pajunoja A., Smith J.N., Lehtinen K.E.J., Worsnop D.R., Laaksonen A. & Virtanen A. 2014. Atmospheric submicron aerosol composition and particulate organic nitrate formation in a boreal forestland-urban mixed region. *Atmos. Chem. Phys.* 14: 13483–13495.
- Haywood J.M. & Boucher O. 2000. Estimates of the direct and in-direct radiative forcing due to tropospheric aerosols: a review. *Rev. Geophys.* 38: 513–543.
- Hari P. & Kulmala M. 2005. Station for measuring ecosystem-atmosphere relations (SMEAR II). *Boreal Env. Res.* 10: 315–322.
- IPCC 2013. *Climate change 2013: The physical science basis*. Contribution of Working Group I to the Fifth Assessment Report of the Intergovernmental Panel on Climate Change, Cambridge University Press, Cambridge, United Kingdom and New York, NY, USA.
- Jayne J.T., Leard D. C., Zhang X., Davidovits P., Smith K.A., Kolb C.E. & Worsnop D.R. 2000. Development of an Aerosol Mass Spectrometer for size and composition analysis of submicron particles. *Aerosol Sci. Technol.* 33: 49–70.
- Jimenez J.L., Jayne J.T., Shi Q., Kolb C.E., Worsnop D.R., Yourshaw I., Seinfeld J.H., Flagan R. C., Zhang X., Smith K.A., Morris J.W. & Davidovits P. 2003. Ambient aerosol sampling using the aerodyne aerosol mass spectrometer. *J. Geophys. Res.* 108(D7), 8425, doi:10.1029/2001JD001213.
- Junninen H., Lauri A., Keronen P., Aalto P., Hiltunen V., Hari P. & Kulmala M. 2009. Smart-SMEAR: on-line data exploration and visualization tool for SMEAR stations. *Boreal Env. Res.* 14: 447–457.
- Kulmala M. 2003. How particles nucleate and grow. *Science* 302: 1000–1001.
- Kulmala M., Vehkamäki H., Petäjä T., Dal Maso M., Lauri A., Kerminen V.-M., Birmili W. & McMurry P.H. 2004. Formation and growth rates of ultrafine atmospheric particles: a review of observations. *J. Aerosol. Sci.* 35:

- 143–176.
- Liao L., Dal Maso M., Taipale R., Rinne J., Ehn M., Junninen H., Äijälä M., Nieminen T., Alekseychik P., Hultkko-nen M., Worsnop D.R., Kerminen V.-M. & Kulmala M. 2011. Monoterpene pollution episodes in a forest environment: indication of anthropogenic origin and association with aerosol particles. *Boreal Env. Res.* 16: 288–303.
- Lindfors V. & Laurila T. 2000. Biogenic volatile organic compound (VOC) emissions from forests in Finland. *Boreal Env. Res.* 5: 95–113.
- Liu S., Shilling J.E., Song C., Hiranuma N., Zaveri R.A. & Russell L.M. 2012. Hydrolysis of organonitrate functional groups in aerosol particles. *Aerosol Sci. Technol.* 46: 1359–1369.
- McMurry P.H., Takano H. & Anderson G.R. 1983. Study of the ammonia (gas)–sulphuric acid (aerosol) reaction rate. *Environ. Sci. Technol.* 17: 347–352.
- Murphy J.G., Day D.A., Cleary P.A., Wooldridge P.J. & Cohen R.C. 2006. Observations of the diurnal and seasonal trends in nitrogen oxides in the western Sierra Nevada. *Atmos. Chem. Phys.* 6: 5321–5338.
- Middlebrook A.M., Bahreini R., Jimenez J.L. & Canagaratna M.R. 2012. Evaluation of composition-dependent collection efficiencies for Aerodyne Aerosol Mass Spectrometer using field data. *Aerosol Sci. Technol.* 46: 258–271.
- Ng N.L., Canagaratna M.R., Zhang Q., Jimenez J.L., Tian J., Ulbrich I.M., Kroll J.H., Docherty K.S., Chhabra P.S., Bahreini R., Murphy S.M., Seinfeld J.H., Hildebrandt L., Donahue N.M., DeCarlo P.F., Lanz V.A., Prévôt A.S.H., Dinar E., Rudich Y. & Worsnop D.R. 2010. Organic aerosol components observed in Northern Hemispheric datasets measured with aerosol mass spectrometry. *Atmos. Chem. Phys.* 10: 4625–4641.
- Paatero P. & Tapper U. 1994. Positive matrix factorization: a non-negative factor model with optimal utilization of error estimates of data values. *Environmetrics* 5: 111–126.
- Paatero P. 1997. Least squares formulation of robust non-negative factor analysis. *Chemometr. Intell. Lab.* 37: 23–35.
- Pennington M.R., Bzdek B.R., DePalma J.W., Smith J.N., Kortelainen A., Hildebrandt R.L., Petäjä T., Kulmala M., Worsnop D.R. & Johnston M.V. 2013. Identification and quantification of particle growth channels during new particle formation. *Atmos. Chem. Phys.* 13: 1680–7316.
- Pye H.O.T., Chan A.W.H., Barkley M.P. & Seinfeld J.H. 2010. Global modeling of organic aerosol: the importance of reactive nitrogen ( $\text{NO}_x$  and  $\text{NO}_3$ ). *Atmos. Chem. Phys.* 10: 11261–11276.
- Quinn P.K., Bates T.S., Coffman D., Onasch T.B., Worsnop D., Baynard T., de Gouw J.A., Goldan P.D., Kuster W.C., Williams E., Roberts J.M., Lerner B., Stohl A., Pettersson A. & Lovejoy E.R. 2006. Impacts of sources and aging on submicrometer aerosol properties in the marine boundary layer across the Gulf of Maine. *J. Geophys. Res.* 111, D23S36, doi:10.1029/2006jd007582.
- Raatikainen T., Vaattovaara P., Tiitta P., Miettinen P., Rautiainen J., Ehn M., Kulmala M., Laaksonen A. & Worsnop D.R. 2010. Physicochemical properties and origin of organic groups detected in boreal forest using an aerosol mass spectrometer. *Atmos. Chem. Phys.* 10: 2063–2077.
- Rindelaub J.D., McAvey K.M. & Shepson P.B. 2014. Determination of  $\alpha$ -pinene-derived organic nitrate yields: particle phase partitioning and hydrolysis. *Atmos. Chem. Phys. Discuss.* 14: 3301–3335.
- Roberts J.M. 1990. The atmospheric chemistry of organic nitrates. *Atmos. Environ.* 24A: 243–287.
- Rollins A.W., Fry J.L., Hunter J.F., Kroll J.H., Worsnop D.R., Singaram S.W. & Cohen R.C. 2010. Elemental analysis of aerosol organic nitrates with electron ionization high-resolution mass spectrometry. *Atmos. Meas. Tech.* 3: 301–310.
- Rollins A.W., Browne E. C., Min K.-E., Pusede S.E., Wooldridge P.J., Gentner D.R., Goldstein A.H., Liu S., Day D.A., Russell L.M. & Cohen R.C. 2012. Evidence for  $\text{NO}_x$  control over nighttime SOA formation. *Science* 337: 1210–1212.
- Rolph G.D. 2013. *Real-time Environmental Applications and Display sYstem (READY)*. NOAA Air Resources Laboratory, College Park, MD. [Available at <http://www.ready.noaa.gov>].
- Russell L.M., Bahadur R. & Ziemann P.J. 2011. Identifying organic aerosol sources by comparing functional group composition in chamber and atmospheric particles. *Proc. Natl. Acad. Sci. USA* 108: 3516–3521.
- Tarvainen V., Hakola H., Rinne J., Hellén H. & Haapanala S. 2007. Towards a comprehensive emission inventory of terpenoids from boreal ecosystems. *Tellus* 59B: 526–534.
- Ulbrich I.M., Canagaratna M.R., Zhang Q., Worsnop D.R. & Jimenez J.L. 2009. Interpretation of organic components from positive matrix factorization of aerosol mass spectrometric data. *Atmos. Chem. Phys.* 9: 2891–2918.
- Virkkula A., Mäkelä T., Hillamo R., Yli-Tuomi T., Hirsikko A., Hämeri K. & Koponen I.K. 2007. A simple procedure for correcting loading effects of aethalometer data. *J. Air Waste Manage. Assoc.* 57: 1214–1222.
- Zaveri R.A., Berkowitz C.M., Brechtel F.J., Gilles M.K., Hubbe J.M., Jayne J.T., Kleinman L.I., Laskin A., Madronich S., Onasch T.B., Pekour M.S., Springston S.R., Thornton J.A., Tivanski A.V. & Worsnop D.R. 2010. Nighttime chemical evolution of aerosol and trace gases in a power plant plume: implications for secondary organic nitrate and organosulfate aerosol formation,  $\text{NO}_3$  radical chemistry, and  $\text{N}_2\text{O}_5$  heterogeneous hydrolysis. *J. Geophys. Res.* 115, D12304, doi: 10.1029/2009JD013250.
- Zhang Q., Canagaratna M.R., Jayne J.T., Worsnop D.R. & Jimenez J.L. 2005. Time- and size-resolved chemical composition of submicron particles in pittsburgh: implications for aerosol sources and processes. *J. Geophys. Res.* 110, D07s09, doi:10.1029/2004jd004649.